

Kinetics of Isothermal Crystallization and Subsequent Melting Behavior of PTT/PA12 Blend

A. Asadinezhad,¹ S. H. Jafari,¹ H. A. Khonakdar,² F. Böhme,³ R. Hässler,³ L. Häussler³

¹School of Chemical Engineering, University College of Engineering, University of Tehran, Tehran, Iran

²Iran Polymer and Petrochemical Institute (IPPI), P.O. Box 14965/115, Tehran, Iran

³Leibniz Institute of Polymer Research Dresden, Dresden D-01069, Germany

Received 4 March 2007; accepted 6 May 2007

DOI 10.1002/app.26808

Published online 20 July 2007 in Wiley InterScience (www.interscience.wiley.com).

ABSTRACT: The kinetics of isothermal crystallization along with subsequent melting behavior of melt-mixed immiscible binary blends of poly(trimethylene terephthalate) (PTT) and polyamide-12 (PA12) were investigated by means of differential scanning calorimetry. Three macrokinetic models of Avrami, Tobin, and Malkin were used which could adequately describe isothermal crystallization kinetics of the blends as well as the neat components. However, the commonly used Avrami model provided more consistent data for the system of interest. Based on the half-time of crystallization, one could conclude that PTT crystallizes more rapidly than PA12. The kinetic parameters suggested that blending had a distinct influence on reducing the rate of isothermal crystallization particu-

larly at medium degrees of undercooling. From reciprocal crystallization half-time, it was concluded that over the temperature range covered; the samples crystallized inside the nucleation-controlled region. The secondary nucleation mechanism generally prevailed in the PA12 isothermal crystallization whereas in PTT, the primary crystallization mechanism dominated. With respect to the position of melt transitions, blending was proven to exert only small effects, however, it reduced the crystallinity of both constituents particularly that of PA12 significantly. © 2007 Wiley Periodicals, Inc. *J Appl Polym Sci* 106: 1964–1971, 2007

Key words: poly(trimethylene terephthalate); polyamide-12; blends; crystallization; melting behavior

INTRODUCTION

The challenging subject of polymer blends crystallization has been of great concern for the recent years and still provides fruitful areas of research. Crystallization, similar to other phase transformations, follows the laws of thermodynamics which determine whether under specific conditions, crystals may form or not. Additionally, whether crystallization can take place, is governed by the kinetics of the process.¹

Nucleation and growth are the most dominant processes known to date for crystallization from the molten state. The kinetics of nucleation and growth, mainly influenced by temperature, pressure, and time, can be analyzed by means of isothermal techniques in which the crystallization course is specifically investigated at defined temperatures and described by relevant macrokinetic models.^{2,3}

In immiscible blend systems, interactions between the components as well as phase separation phenomena may influence the primary effects of crystallization as for example nucleation and growth rate.

On the basis of the literature,² the following processes have learnt to be at work: first, nucleation of the slower crystallizing component on already-formed crystals of the faster crystallizing component as observed in poly(phenylene sulfide)/poly(ethylene terephthalate)^{4,5} and poly(vinylidene fluoride)/polypropylene blends⁶; second, retardation of the nucleation of the higher melting species by the lower melting species at continuous cooling reported for polypropylene/high-density polyethylene⁷ or poly(ethylene terephthalate)/high density polyethylene blends⁸; third, increase of the nucleation rate of the higher melting component by blending with a lower melting component at relatively high undercooling; and fourth, enhanced nucleation rate of a higher melting component by blending of a lower melting component. At the same time, either increasing or decreasing of the growth rate can be observed. An example of an enhanced nucleation rate is the poly(phenylene sulfide)/high-density polyethylene blend.⁹ Nevertheless, further attempts are to be made in order to understand the crystallization behavior of incompatible blends completely.

In our earlier publications,^{10,11} it was reported that poly(trimethylene terephthalate) (PTT), a recent aromatic polyester with an interesting combination of prominent properties,¹² and polyamide-12 (PA12) are intrinsically immiscible showing a droplet

Correspondence to: S. H. Jafari (shjafari@ut.ac.ir).

Contract grant sponsor: Iran National Science Foundation (INSF).

morphology where polyamide forms the minor phase. The nonisothermal crystallization of the system and its melting behavior was also studied.¹⁰ The current article focuses on the kinetics of isothermal crystallization of PTT/PA12 blends by means of different macrokinetic models typically used to describe immiscible systems. Furthermore, the melting behavior of isothermally crystallized samples is explored.

THEORETICAL BASIS

Based on the assumption that the development of crystallinity is proportional to the evolution of heat released within the crystallization course, one may gain knowledge on the crystallization kinetics of polymer systems by analyzing the respective crystallization exotherms.¹³ The relative crystallinity (θ_t) as a function of crystallization time (t) is defined as follows,¹⁴

$$\theta(t) = \frac{\int_0^t (dH_c/dt)dt}{\int_0^\infty (dH_c/dt)dt} = \frac{\Delta H_t^c}{\Delta H_{t=\infty}^c} \quad (1)$$

in which t and ∞ are the elapsed time during the crystallization and at the end of crystallization process, respectively, and dH_c is the enthalpy of crystallization during an infinitesimal time interval dt . $\Delta H_{t=\infty}^c$ and ΔH_t^c denote the crystallization enthalpies at complete crystallization and after time t , respectively.

A number of macrokinetic models^{14–20} have been proposed to quantitatively describe the macroscopic evolution of crystallization under quiescent isothermal conditions, the most popular of which are those of Avrami,^{15–17} Tobin,^{18–20} and Malkin.²¹ In the first model, the following equation links the relative crystallinity with the crystallization time exponentially as follows,

$$\theta(t) = 1 - \exp[-k_a t^{n_a}] \quad (2)$$

where k_a and n_a are the Avrami crystallization rate coefficient and the Avrami exponent, respectively. Both k_a and n_a are characteristic values for the particular crystalline morphology and nucleation type under the specific crystallization conditions applied.²²

Tobin suggested a different expression to explain the relationship between the relative crystallinity and the crystallization time by taking the growth impingement concept into consideration. The original theory was written in the form of a non-linear integral equation, the zeroth order solution of which leads to:

$$\theta(t) = \frac{k_t t^{n_t}}{1 + k_t t^{n_t}} \quad (3)$$

where k_t is the Tobin rate coefficient and n_t is the Tobin exponent. Based on this proposition, the Tobin expo-

nent is mainly governed by the different types of nucleation and growth mechanisms. This model, compared to the former one, better describes the later stages of the crystallization.^{2,3}

Malkin developed an equation including the postulation that the total rate of crystallization is basically affected by the appearance of primary nuclei and alterations of the crystal growth rate during crystallization. This model is as follows,

$$\theta(t) = 1 - \frac{C_0 + 1}{C_0 + \exp(C_1 t)} \quad (4)$$

where C_0 is the Malkin exponent which is directly connected with the ratio of crystal growth rate, G , to the primary nucleation rate, I , and C_1 is the Malkin crystallization rate coefficient directly related to the overall crystallization, i.e. $C_1 = aG + bI$, where a and b are specific constants. The unit of C_1 is given in (time)⁻¹.

EXPERIMENTAL

Materials

PTT with the trade name CORTERRA[®] grade 200 and a mass density of 1.33 g/cm³, was supplied by Shell Chemicals. The intrinsic viscosity of PTT measured at 25°C in a 60/40 mixture of phenol and tetrachloroethane was 0.9 mL/g. PA12 available as Grilamid[®], grade L25, with a weight and number average molecular weights of 60,000 g/mol and 31,000 g/mol, respectively, and a mass density of 1.01 g/cm³ was received from EMS-CHEMIE. To reduce the moisture content to the lowest possible level, both constituents were dried for 24 h at 80°C under vacuum before melt blending.

Blend preparation

Melt blends of PTT and PA12 in compositions PTT/PA12 75/25 and 90/10 (w/w) were prepared by means of a conical twin-screw microcompounder (DACA), at a mixing time of 10 min, a screw speed of 100 rpm, and a temperature of 230°C. The homogeneity of the samples was ensured via monitoring the torque values of the mixer against the blending time.

Isothermal crystallization measurements

Differential scanning calorimetry (DSC) measurements were performed on a Q1000 DSC (TA Instruments) with samples of about 10 mg sealed in aluminum pans under nitrogen atmosphere. For the isothermal crystallization analysis, first, the samples were heated at the rate of 10 K/min to a melt temperature of 250°C, and kept there for 2 min in order to erase thermal history. In the second step, the sam-

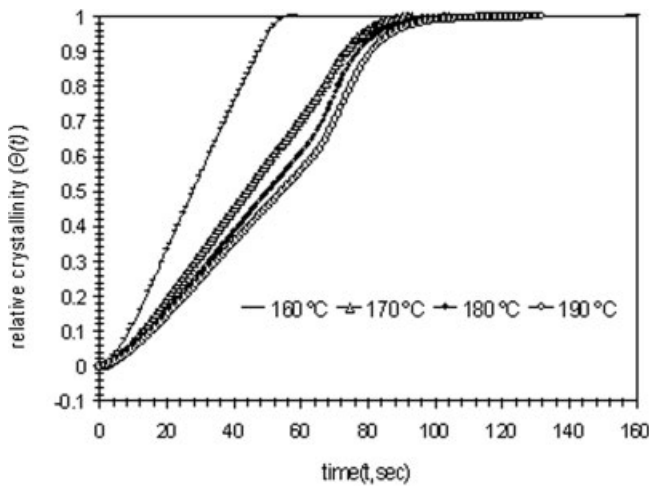


Figure 1 Relative crystallinity versus time for neat PTT at four crystallization temperatures.

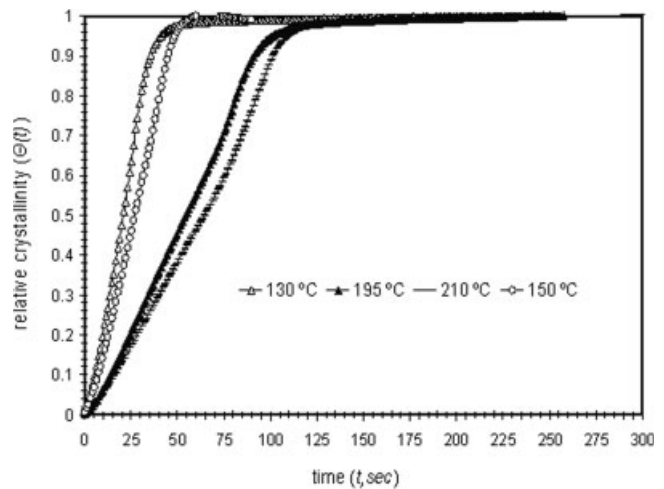


Figure 3 Relative crystallinity versus time for PTT/PA12 (75/25) at four crystallization temperatures.

ples were cooled down to the defined isothermal crystallization temperatures (T_{iso}) at the rate of 40 K/min. The samples were held at the chosen isothermal crystallization temperatures until crystallization was completed (no significant change in heat flow). After each isothermal crystallization time interval, the melting behavior was recorded with a heating rate of 10 K/min to 250°C. The respective crystallinity of the individual phases (X_c) was calculated from the melting enthalpies (ΔH_m -neglecting its variation with temperature over the range studied) in terms of the following relation:

$$X_c = \frac{\Delta H_m}{w_c \Delta H_m^o} \times 100 \quad (5)$$

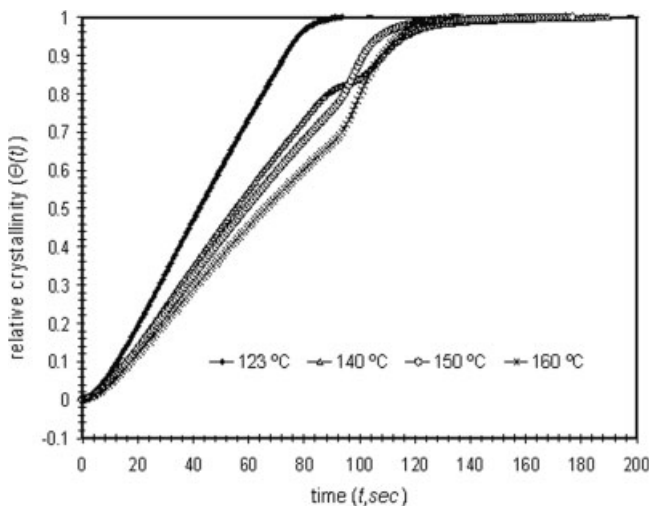


Figure 2 Relative crystallinity versus time for neat PA12 at four crystallization temperatures.

where w_c is the mass fraction and ΔH_m^o the maximum melting enthalpy (100% crystallinity) of the respective component based on literature data (for pure PTT,¹² $\Delta H_m^o = 140$ J/g and for pure PA12,²³ $\Delta H_m^o = 233.5$ J/g). The Universal Analysis[®] 2000 software (TA Instruments) was also employed to further analyze our experimental data.

RESULTS AND DISCUSSION

Analysis of isothermal melt-crystallization data

Isothermal crystallization of PTT and PA12 was performed at different temperatures. The respective time-dependent relative crystallinity functions calculated according to eq. (1) (after discarding the induc-

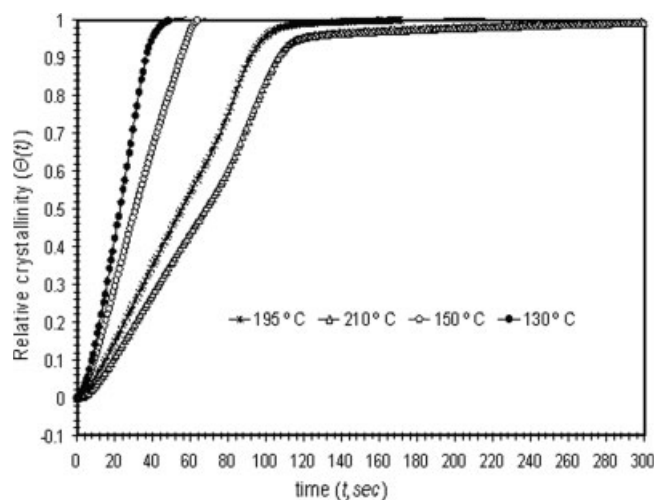


Figure 4 Relative crystallinity versus time for PTT/PA12 (90/10) at four crystallization temperatures.

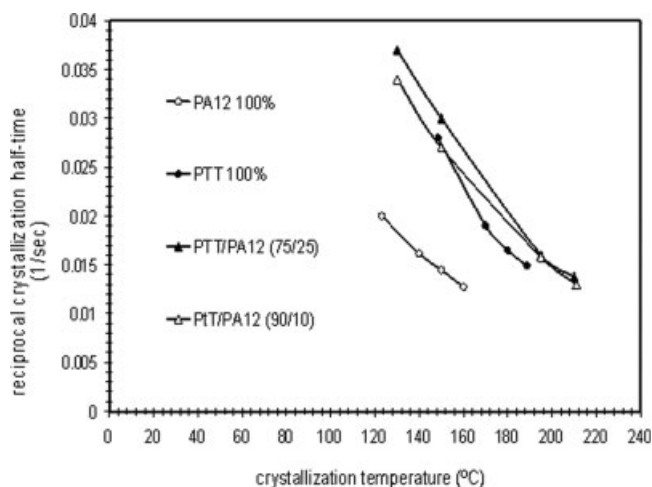


Figure 5 Variation of reciprocal crystallization half-time with crystallization temperature.

tion period) are shown in Figures 1 and 2. Both graphs give an impression of the volume fraction of the polymer transformed into the crystalline front. Within the range of temperature examined, it is evident from both figures that the time to reach maximum crystallinity ($\theta(t) = 1.0$) rises with increasing annealing temperature (T_{iso}). In other words, the degree of undercooling, i.e., the difference between the melting point and T_{iso} , considered as the driving force of the crystallization process, effectively contributes to the isothermal crystallization rate, as frequently mentioned in other reports.^{3,14,24}

Figures 3 and 4 show the relative crystallinity variation with time for the two binary blends, PTT/PA12 (75/25) and PTT/PA12 (90/10), respectively. In both cases, a similar behavior as for the neat constituents was observed. Increasing of annealing temperatures caused an extension of the crystallization time to reach maximum crystallinity. This increase, to some extent, is proportional to the degree of undercooling. It is worth mentioning that at 210°C and 195°C, the PA12 phase exists in the molten state, hence the change of relative crystallinity as stated rather resembles that of neat PTT.

As a matter of fact, $\theta(t)$ is proportional to the product of the material volume fraction present in spherulites and the volume fraction crystallinity within each spherulite behind the primary growth

front. The former is driven by the primary nucleation and the latter is caused by secondary nucleation. In other words, the trend of $\theta(t) - t$ graph is affected by the crystallization regimes. Thus, the changes in the slope of most curves, particularly at lower degree of undercooling, can be ascribed to the regime changes.²

A significant kinetic parameter is the crystallization half-time ($t_{0.5}$), defined as the elapsed time from the onset of crystallization to the point in which crystallinity attains one-half of the complete level. This can be acquired straight from $\theta(t) - t$ plots. Based on Figures 1 and 2, for neat PTT, the half-time of crystallization increases from 36 to 63 s as the isothermal crystallization temperature increases from 160 to 190°C. The same trend is observed for neat PA12, i.e., $t_{0.5}$ climbs up from 50 to 74 s if T_{iso} increases from 123 to 160°C giving credence to the fact that PTT crystallizes more rapidly. This has also been confirmed by our non-isothermal crystallization studies.²⁵ According to Figures 3 and 4, $t_{0.5}$ of PTT/PA12 (75/25) and PTT/PA12 (90/10) increase from 27 to 71 s and 29 to 74 s, respectively, as the isothermal crystallization temperature is increased from 130 to 210°C. The slight difference between the crystallization rate of PTT/PA12 (75/25) and PTT/PA12 (90/10) can be associated with the phase domain size concept. As reported elsewhere,¹¹ the average dispersed phase domains size of the latter blend is smaller than that of the former one leading to a slower rate of PA12 crystallization inside the matrix (PTT) of the latter. This has already been stated in the literature^{26,27} and refers to the presence of less active nuclei inside the smaller domains.

A convenient index for the crystallization rate is the reciprocal crystallization half-time ($1/t_{0.5}$).

Figure 5 displays $1/t_{0.5}$ values of all samples versus T_{iso} which is often considered as the most fundamental representation of isothermal crystallization kinetics of crystallizable polymers.² Concerning this figure, it is seen that upon rising of the isothermal crystallization temperature, the reciprocal crystallization half-time descends exponentially supposed to be part of the typical bell-shaped curve. The bell-shaped curve is an outcome of the competition between the crystallization driving force and the macromolecular mobility and actually has a

TABLE I
Isothermal Crystallization Kinetic Data Based on Avrami Macrokinetic Model

PTT			PA12			PTT/PA12 (75/25)			PTT/PA12 (90/10)		
T_{iso} (°C)	n_a	k_a	T_{iso} (°C)	n_a	k_a	T_{iso} (°C)	n_a	k_a	T_{iso} (°C)	n_a	k_a
160	1.67	0.0032	123	1.69	0.0016	130	1.41	0.0110	130	1.87	0.0026
170	1.70	0.0015	140	1.64	0.0011	150	1.58	0.0050	1	1.61	0.0013
180	1.80	0.0008	150	1.70	0.0008	195	1.56	0.0020	195	1.71	0.0010
190	1.88	0.0006	160	1.64	0.0009	210	1.59	0.0012	210	1.67	0.0008

TABLE II
Isothermal Crystallization Kinetic Data Based on Tobin Macrokinetic Model

PTT			PA12			PTT/PA12 (75/25)			PTT/PA12 (90/10)		
T_{iso} (°C)	n_t	k_t	T_{iso} (°C)	n_t	k_t	T_{iso} (°C)	n_t	k_t	T_{iso} (°C)	n_t	k_t
160	1.83	0.0027	123	1.83	0.0013	130	1.58	0.0100	130	1.99	0.0023
170	1.83	0.0012	140	1.86	0.0008	150	1.65	0.0050	150	1.78	0.0016
180	1.88	0.0008	150	1.75	0.0009	195	1.74	0.0012	195	1.76	0.0011
190	1.88	0.0006	160	1.72	0.0008	210	1.70	0.0010	210	1.90	0.0004

nucleation-controlled character.^{3,28} Accordingly, it is concluded from Figure 5 that over the temperature range covered; the samples crystallize inside the nucleation-controlled region. A less strong temperature dependence of $t_{0.5}$ is characteristic for the secondary nucleation mechanism while a stronger dependence indicates the domination of the primary nucleation mechanism.²² Thus, on the basis of Figure 5; the secondary nucleation mechanism generally prevails in the pure PA12 isothermal crystallization whereas in pure PTT the primary crystallization mechanism dominates. On the other hand, as observed from this figure, the crystallization half-time values of the blends are generally smaller than these of the pure components implying that blending in this system contributes to the rate of isothermal crystallization particularly at medium undercooling.

Application of macrokinetic models to the experimental data

It is useful to employ analyses which concern the isothermal crystallization behavior so fundamental in nature that one can input material constants and output realistic isothermal crystallization kinetics. Accordingly, Avrami model [eq. (2)] has been applied to the experimental data and the results of the best possible fit are summarized in the Table I. k_a characterizes the geometry of the crystal growth front known as Avrami rate constant and n_a which denotes the Avrami exponent, characterizes the dimensionality of the crystal growth front.³ However, the values of n_a rather fluctuate over different isothermal crystallization temperatures, nevertheless the Avrami rate constant values show a sensible trend in such a way that upon increasing T_{iso} , the

values of k_a decrease which is an indicative of a lower rate of isothermal crystallization and is in good agreement with the results stated above. The range, inside which the fractional values of n_a fall, implies a two-dimensional growth mechanism accompanied by a sequence of thermal and athermal nucleation. In fact, this type of combinational nucleation causes the n_a values to be fractional.²⁹

The second analysis based on the Tobin model can be carried out by fitting the experimental data obtained to eq. (3). As demonstrated in Table II, the values of n_t and k_t exhibit the same trend as the former model regarding this fact that n_t and k_t bear the same meaning as n_a and k_a . However, the values of n_t have been found to be slightly higher than n_a which originates from the model assumptions. The n_t values are fractional similar to n_a suggesting that the nucleation process is a combination of thermal and athermal mechanisms. Increasing in T_{iso} , as expected, brings about a reduction in the Tobin rate constant (k_t) putting emphasis on the notion that decreasing T_{iso} is favorable to the overall isothermal crystallization rate.

Despite the two former models, there is no analytical procedures to directly calculate the constants specific to the Malkin model [eq. (4)], i.e., C_0 and C_1 directly. Therefore, using the set of following equations which provides a correlation between the Avrami and Malkin constants serves this purpose:²¹

$$C_0 = 4^{n_a} - 4 \quad (6)$$

$$C_1 = \frac{\ln(C_0 + 2)k_a}{\ln 2^{n_a}} \quad (7)$$

Table III gives the values of C_0 and C_1 of all samples at different T_{iso} . According to this table,

TABLE III
Isothermal Crystallization Kinetic Data Based on Malkin Macrokinetic Model

PTT			PA12			PTT/PA12 (75/25)			PTT/PA12 (90/10)		
T_{iso} (°C)	C_0	C_1	T_{iso} (°C)	C_0	C_1	T_{iso} (°C)	C_0	C_1	T_{iso} (°C)	C_0	C_1
160	6.12	0.0124	123	6.41	0.0063	130	3.08	0.0300	130	9.36	0.0125
170	6.56	0.0060	140	5.71	0.0041	150	4.94	0.0173	150	5.32	0.0047
180	8.13	0.0036	150	6.56	0.0032	195	4.69	0.0067	195	6.70	0.0040
190	9.55	0.0029	160	5.71	0.0034	210	5.06	0.0042	210	6.13	0.0031

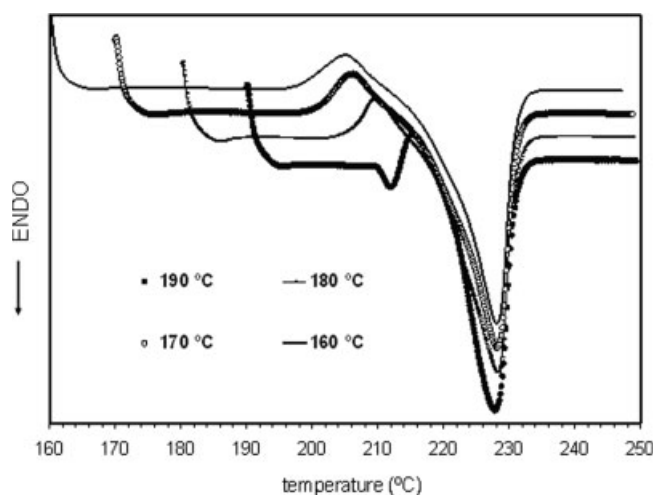


Figure 6 Subsequent melting endotherms of isothermally-crystallized neat PTT samples at different temperatures.

parameter C_1 shows the temperature dependence in a similar manner as the crystallization rate constants characteristic of both the Avrami and Tobin models giving credence to the results stated so far. Also the fractional values of C_0 follow the same fluctuating trend of n_a . Comparing the model predictions of the experimental data, one may conclude that the three models describe the isothermal melt-crystallization behavior of the samples seemingly well in a similar manner. However, the Avrami model seems to be more convenient since it gives more consistent data for the system of interest.

Subsequent melting behavior of pure components

Figure 6 shows the subsequent melting endotherms of the isothermally crystallized PTT. A multiple

melting behavior is observed in the heating plots of neat PTT. This multiplicity actually results from the melting of crystallites with different thermodynamic stability.^{3,30} However, upon decreasing the crystallization temperature from 190 to 160 °C, the magnitude of the minor peak decreases whereas the shape and the intensity of the main melting peak remains unchanged. Also, PTT shows a cold crystallization peak ($T_{c,c}$), associated with reorganization of PTT chains, which is in general accordance with other reports.³¹ Further, the width and the intensity of the cold crystallization peak increase as T_{iso} decreases. This shows that crystallization is inhibited at lower annealing temperatures. Obviously, strong undercooling results in the formation of less perfect crystals with amorphous inclusions which start to crystallize during the second heating and cause the cold crystallization phenomenon observed. Thermodynamic data taken from the experiments are summarized in Table IV. After subtracting the enthalpy of cold crystallization from the overall crystallization, it is deduced that the influence of annealing on the crystallinity is detrimental meaning that the percentage of crystallinity obtained via eq. (5) generally enhances as the crystallization temperature decreases. However, this change is not significant. The position of the main melting peak of PTT appears at around 228 °C³² is not influenced by the annealing process whereas the cold crystallization peak shifts to higher temperatures on increasing T_{iso} .

The DSC heating scan of PA12 after isothermal heating at different temperatures is shown in Figure 7. The respective data are summarized in Table IV. The results show that increasing T_{iso} from 123 to 160 °C causes no considerable change in the percentage of crystallinity. Interestingly, shoulders arising on the

TABLE IV
Thermodynamic Data of Isothermally-Crystallized Samples Annealed at Different Temperatures (T_{iso})

Sample	T_{iso} (°C)	T_m (°C) (main peak)		ΔH_m (J/g)		% X_c		$T_{c,c}$ (°C)	
		PTT	PA12	PTT	PA12	PTT	PA12	PTT	PA12
PTT	160	228.0	–	49.5	–	35	–	205.0	–
	170	228.1	–	49.3	–	35	–	206.0	–
	180	228.1	–	48.2	–	34	–	209.5	–
	190	227.8	–	44.2	–	31	–	215.4	–
PA12	123	–	178.8	–	41.5	–	18	–	–
	140	–	178.8	–	42.3	–	19	–	–
	150	–	178.6	–	43.6	–	20	–	–
	160	–	178.0	–	43.0	–	19	–	–
PTT/PA12 (75/25)	130	227.3	177.8	33.3	9.1	32	15.6	200.0	–
	150	227.4	178.0	33.2	3.9	32	6.7	200.0	–
	195	227.7	–	26.0	–	25	–	218.9	–
	210	223.2	–	1.2	–	1.1	–	–	–
PTT/PA12 (90/10)	130	226.3	176.2	41	3.3	32	14	198.3	–
	150	226.4	177.1	40.8	1.8	32	7.8	198.0	–
	195	227.0	–	38.6	–	30	–	228.1	–
	210	222.6	–	1.2	–	1	–	–	–

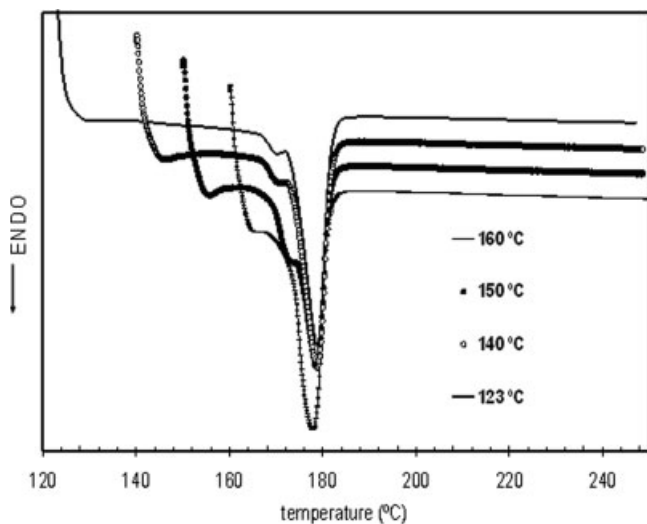


Figure 7 Subsequent melting endotherms of isothermally-crystallized neat PA12 samples.

left-hand side of the main peak, within the range from 145 to 173°C, are indicative of multiple melting behavior of neat PA12 which diminish upon decreasing T_{iso} . The sample annealed at 160°C does not show this behavior. The main melting peak, as reported before,¹⁰ arises around 178°C. No cold crystallization behavior is observed in case of neat PA12 signifying that PA12 chains do not take part in any reorganization processes during the heating scan.

Subsequent melting behavior of PTT/PA12 (75/25) and (90/10) blends

DSC curves of the PTT/PA12 (75/25) and PTT/PA12 (90/10) blends obtained after isothermal annealing are illustrated in Figures 8 and 9, respectively. Taking into account that the PA12 phase exists in the molten state at 210 and 195°C, it becomes clear that the total crystallinity of the blends after annealing at these two temperatures is significantly lower than after annealing at 130 and 150°C. Upon increasing T_{iso} from 195 to 210°C, the percentage of crystallinity of PTT decreases intensely. Blending does not change the main melting points of the components significantly but has a distinct influence on their crystallinity (see Table IV). The melting enthalpy of both compounds, especially that of PA12, is distinctly reduced in both blends compared to the values obtained for the pure components.

It is interesting to note that the cold crystallization of PTT becomes more pronounced if T_{iso} decreases to 130°C which is consistent with the observations about neat PTT. Increasing T_{iso} shifts $T_{c,c}$ of PTT to higher temperatures. Furthermore, the cold crystallization peak of PTT in the blends is shifted to lower

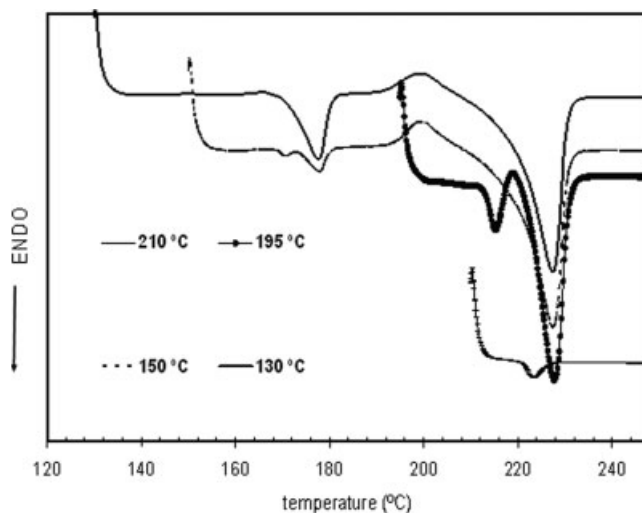


Figure 8 Subsequent melting endotherms of isothermally-crystallized PTT/PA12 (75/25) samples.

temperatures which can be explained by a plasticizing effect (physical interaction) of PA12 chains on PTT chains. The DSC curve of the blends obtained after annealing at 210°C neither shows cold crystallization nor multiple melting behavior. The melting transition of PTT is shifted to lower temperatures (223°C) and appears very weak. Obviously, crystallization does not take place in larger extent at this temperature.

CONCLUSIONS

On the basis of DSC measurements, the isothermal crystallization kinetics of PTT/PA12 binary immiscible blends was discussed by means of three macrokinetic models. It could be shown that the three models describe the crystallization behavior of the blends

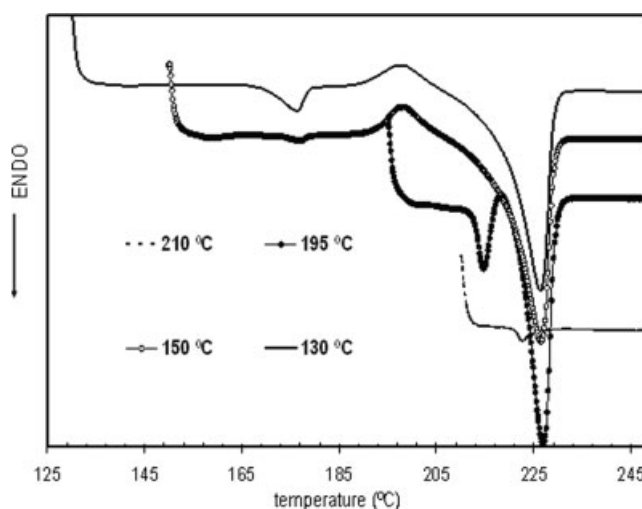


Figure 9 Subsequent melting behavior of isothermally-crystallized PTT/PA12 (90/10) samples.

in an adequate manner, however, with reference to the Avrami model which provides more consistent data for the system of interest. It is found that on increasing the isothermal temperature of crystallization, the rate of crystallization decreases. This concerns the individual components and the polymer blends as well. Based on the half-time of crystallization, one can conclude that PTT crystallizes more rapidly than PA12. The results show that blending has a distinct influence on the rate of isothermal crystallization particularly at medium degrees of undercooling. It is observed that over the temperature range covered; the samples crystallize inside the nucleation-controlled region. With respect to the position of melt transitions, blending has proven to exert only small effects but reduces the crystallinity of both constituents particularly that of PA12 significantly. Also, the total crystallinity of PTT/PA12 (75/25) is relatively higher than that of PTT/PA12 (90/10).

References

1. Di Lorenzo, M. L.; Silvestre, C. *Prog Polym Sci* 1999, 24, 917.
2. Shultz, J. M. *Polymer Crystallization: The Development of Crystalline Order in Thermoplastic Polymers*; American Chemical Society: Washington, D.C., 2001.
3. Dangseeyun, N.; Srimoan, P.; Supaphol, P.; Nithitanakul, M. *Thermochim Acta* 2004, 409, 63.
4. Nadkarni, V. M.; Shingankuli, V. L.; Jog, I. P. *J Appl Polym Sci* 1992, 46, 339.
5. Shingankuli, V. L.; Jog, J. P.; Nadkarni, V. M. *J Appl Polym Sci* 1994, 51, 1463.
6. Nadkarni, V. M. Jog J. P. In *Two-Phase Polymer Systems*; Utracki, L. A., Ed.; Hanser Publishers: Munich, 1991.
7. Martuscelli, E.; Pracella, M.; Volpe, G. D.; Greco, R.; Ragosta, G. *Macromol Chem* 1980, 181, 957.
8. Bartczak, Z.; Martuscelli, E. *Macromol Chem* 1987, 188, 445.
9. Nadkarni, V. M.; Shingankuli, V. L.; Jog, J. P. *Int Polym Process* 1987, 2, 53.
10. Asadinezhad, A.; Yavari, A.; Jafari, S. H.; Khonakdar, H. A.; Böhme, F.; Hässler, R. *Polym Bull* 2005, 54, 205.
11. Asadinezhad, A.; Yavari, A.; Jafari, S. H.; Khonakdar, H. A.; Böhme, F. *Polym Eng Sci* 2005, 45, 1401.
12. Zhang, J. *J Appl Polym Sci* 2004, 91, 1657.
13. Hay, J. N. *Br Polym J* 1979, 11, 137.
14. Xu, J. T.; Fairclough, P. A.; Mai, S. M.; Ryan, A. J.; Chaibundit, C. *Macromolecules* 2002, 35, 6937.
15. Avrami, M. *J Chem Phys* 1939, 7, 1103.
16. Avrami, M. *J Chem Phys* 1940, 8, 212.
17. Avrami, M. *J Chem Phys* 1934, 9, 1117.
18. Tobin, M. C. *J Polym Sci Part B: Polym Phys* 1974, 12, 399.
19. Tobin, M. C. *J Polym Sci Part B: Polym Phys* 1976, 14, 2253.
20. Tobin, M. C. *J Polym Sci Part B: Polym Phys* 1977, 15, 2269.
21. Malkin, A. Y.; Beghishev, V. P.; Keapin, I. A.; Bolgov, S. A. *Polym Eng Sci* 1984, 24, 1396.
22. Wanderlich, B. *Macromolecular Physics*; Academic Press: New York, 1976.
23. Van Krevelen, D. W. *Properties of Polymers*; Elsevier Science Press: London, 1997.
24. Tol, R. T.; Mathot, V. B. F.; Groeninckx, G. *Polymer* 2005, 46, 2955.
25. Jafari, S. H.; Asadinezhad, A.; Yavari, A.; Khonakdar, H. A.; Böhme, F. *Polym Bull* 2005, 54, 417.
26. Tol, R. T.; Mathot, V. B. F.; Groeninckx, G. *Polymer* 2005, 46, 369.
27. Tang, T.; Lei, Z.; Huang, B. *Polymer* 1996, 37, 3219.
28. Supaphol, P. *Thermochim Acta* 2001, 370, 37.
29. Janeschitz, H.; Rajatski, E.; Wipel, H. *Colloid Polym Sci* 1999, 227, 217.
30. Chung, W. T.; Yeh, W. J.; Hong, P. D. *J Appl Polym Sci* 2002, 83, 2426.
31. Huang, J. M.; Chang, F. C. *J Appl Polym Sci* 2002, 84, 850.
32. Huang, J. M.; Chang, F. C. *J Polym Sci Part B: Polym Phys* 2000, 38, 934.